Journal of Sensor Science and Technology
Vol. 27, No. 5 (2018) pp. 275-279
http://dx.doi.org/10.5369/JSST.2018.27.5.275
pISSN 1225-5475/eISSN 2093-7563

Plasmon-enhanced Infrared Spectroscopy Based on Metasurface Absorber with Vertical Nanogap

Inyong Hwang[1], Jongwon Lee[1], and Joo-Yun Jung[2,+]

Abstract

In this study, we introduce a sensing platform based on a plasmonic metasurface absorber (MA) with a vertical nanogap for the ultra-sensitive detection of monolayer molecules. The vertical nanogap of the MA, where the extremely high near-field is uniformly distributed and exposed to the external environment, is formed by an under-cut structure between a metallic cross nanoantenna and the mirror layer. The accessible sensing area and the enhanced near-field of the MA further enhance the sensitivity of surface-enhanced infrared absorption for the target molecule of 1-octadecanethiol. To provide strong coupling between the molecular vibrations and plasmonic resonance, the design parameters of the MA with a vertical nanogap are numerically designed.

Keywords: Metasurfaces, plasmonics, Surface-enhanced infrared absorption, nanogap

1. INTRODUCTION

Infrared (IR) absorption spectroscopy is a powerful and label-free optical detection method to determine structural properties of various molecules via their IR absorption fingerprint vibrations [1]. IR absorption spectroscopy through IR fingerprint vibrations is used in such fields as pharmacy, safety, food, and general substance identification. However, for molecules with small IR absorption cross-sections such as minute amounts of analyte molecules or very thin samples such as monolayers, conventional IR absorption cannot provide good sensitivity. To address this challenge, surface-enhanced infrared absorption (SEIRA) spectroscopy has been proposed to enhance the IR fingerprint vibrations of molecules in the vicinity of the plasmonic metallic surface through coupling between the fingerprint vibrations of molecules and the enhanced and confined electromagnetic near-fields called hot spots using localized surface plasmon resonance. For applications of SEIRA, numerous plasmonic metallic nanostructures, such as nanodisk, nanosized gap, nanoantennas, metamaterial, and metasurface absorber (MA) have been investigated recently [2-8].

Metasurfaces are a type of thin metamaterial structure comprising an array of sub-wavelength-sized resonators and can produce unique spectral responses through the abrupt changes in the phase and amplitude of the incident electromagnetic wave at the surface of the metal layer from microwave to optical wavelengths [9-12]. The ability of metasurfaces to control and enhance electromagnetic waves at sub-wavelength scale leads to interesting applications, such as hologram [10], lens [11], anomalous reflection and refraction [13], and absorbers [14]. Particularly, metasurfaces have been used as a component of narrowband [15], broadband [16], or tunable so-called perfect absorbers [17]. MAs consist of metallic resonators on top of a metallic mirror layer separated by a thin dielectric spacer layer. Near-unity absorption of MAs at a particular wavelength produces a confined and enhanced electromagnetic near-field between the metallic resonators and the metal mirror owing to the excitation of localized surface plasmon resonance.

To enhance the sensitivity of SEIRA, an important strategy is to maximize the hot spot overlap with the target molecule, which indicates an increased effective sensing area. Approaches that use nanoantennas on dielectric pedestals, where the cross-section of the dielectric pedestals underneath the nanoantenna is smaller than the size of the nanoantenna, provide an increased effective sensing area as they allow access to the bottoms of nanoantennas [4, 5].

In this study, a method for the detection of ultrasensitive molecules based on MAs with vertical nanogaps is numerically

[1]School of Electrical and Computer Engineering, Ulsan National Institute of Science and Technology, Ulsan, 44919, Korea
[2]Nano-convergence Mechanical Systems Research Division, Korea Institute Machinery and Materials, Daejeon, 305-343, Korea
[+]Corresponding author: jjy2121@kimm.re.kr
(Received: Aug. 6, 2018, Accepted: Aug. 25, 2018)

investigated. A vertical nanogap, where the hot spot is uniformly distributed and exposed to the external environment, is formed by an under-cut structure between a metallic cross nanoantenna and the mirror layer. The accessible sensing area of the MAs increases as the cross-section of the dielectric layer beneath the cross nanoantenna decreases. The plasmonic resonance wavelength of the MA can be tuned to the wavelength of the target molecular fingerprint vibrations by adjusting the design parameters of the MA. Using the MAs with vertical nanogaps, a monolayer of molecules of 1-octadecanethiol (ODT) is detected with a highly enhanced SEIRA signal.

2. RESULTS AND DISCUSSIONS

2.1 Design and simulations

Figure 1 (a) and (b) show the schematics of a single unit of the MA and the proposed MA with a vertical nanogap, respectively. The two MAs consist of an array of top gold cross nanoantenna, an Au mirror of thickness 150 nm, and an SiO_2 dielectric spacer layer between the Au layers. The design parameters of the MAs are the dimensions of the cross nanoantenna (length L, width W, and thickness t_1), array period (P), and dimensions of the SiO_2 dielectric layer (thickness t_2, lateral under-cut depth ΔX and ΔY, and vertical under-cut depth ΔZ). For monolayer SEIRA detection, we chose ODT as the target molecule. An ODT molecule shows IR fingerprint vibrations at the wavelengths of 3509 nm and 3427 nm owing to symmetric and asymmetric stretching vibrations of the CH_2 and CH_3 groups, and ODT-coated samples can be prepared on the Au film in the form of a self-assembled monolayer [18]. ODT is a monolayer of a carbon thiol chain with 18 carbon atoms and forms a conformal coated homogeneous layer with a thickness of 2.8 nm on the Au surface [19]. Figure 1 (c) and (d) show the schematic cross-section at the planes of two MAs with ODT coated on the Au layer. The ODT monolayer for MA with a vertical nanogap is formed around the revealed surface of the top Au cross nanoantenna and the surface of the Au mirror layer as shown in Fig. 1 (d). Simulated absorption spectral responses and electric near-fields distributions of MAs were calculated using the commercial finite-difference time domain (FDTD) software Lumerical FDTD-Solutions ver. 8.19. The normal incident plane wave with the electric field polarization along the y-direction excited a single unit of MAs as shown in Fig. 1 (a) and (b) with a periodic boundary condition applied in the x-y plane. The perfectly matched layer boundary

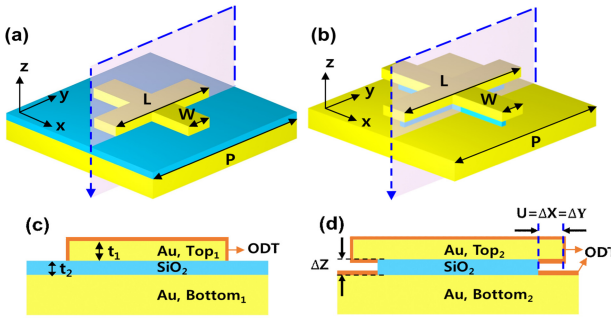

Fig. 1. (a) Schematics of a single unit of MA and (b) MA with a vertical nanogap. (c) The schematic cross-sections of the ODT-coated MA and (d) MA with a vertical nanogap for the plane indicated in (a) and (b)

condition along the z-direction was used. The complex refractive index of the Au layer was described by the Drude model with the plasma frequency ω_p = 1.378×10^{16} rad/s and the collision frequency $\Gamma = 1.224\times10^{14}$ rad/s. The refractive index of SiO_2 was obtained from the Lumerical Palik database and fitted within the simulation wavelength range. To model the ODT IR fingerprint vibrations, the IR refractive index of ODT was used from the literature [20].

2.2 Simulated results and discussions

Figure 2 (a) shows the simulated absorption spectral response of MA as shown in Fig. 1 (a). The simulated MA has the design parameters of P = 1100 nm, L = 900 nm, W = 200 nm, t_1 = 50 nm, and t_2 = 40 nm, and the plasmonic resonance of the MA is at a wavelength of 3570 nm with 92% absorption. Figure 2 (b) shows the simulated absorption spectral responses of the MA with a vertical nanogap for different under-cut depths. The simulated MA with a vertical nanogap has the design parameters of P = 1300 nm, L = 1070 nm, W = 200 nm, t_1 = 50 nm, and t_2 = 40 nm, and the absorption resonance peak of the unetched MA is initially located at a wavelength of 4200 nm. As the under-cut depth increases, the absorption resonance peak shifts to a shorter wavelength owing to the reduction in the effective refractive index of the dielectric spacer layer. The plasmonic resonance of the MA with a vertical nanogap, whose dimensions are $\Delta X = \Delta Y$ = 70 nm and ΔZ = 40 nm, is at a wavelength of 3380 nm. Owing to a higher sensitivity to the external refractive index caused by the increase in the effective sensing area of the MA with a vertical nanogap, the coating of the ODT on the MA with a vertical nanogap produces a higher red-shift of resonance wavelength than the coating of the ODT on the MA. Therefore, the MA with a vertical nanogap is designed to have its absorption resonance peak

at a shorter wavelength compared with that of the MA.

Figure 3 (a) and (b) show the cross-sectional views of the electric near-field distributions of the MA as shown in Fig. 1 (a) and the MA with a vertical nanogap as shown in Fig. 1 (b),

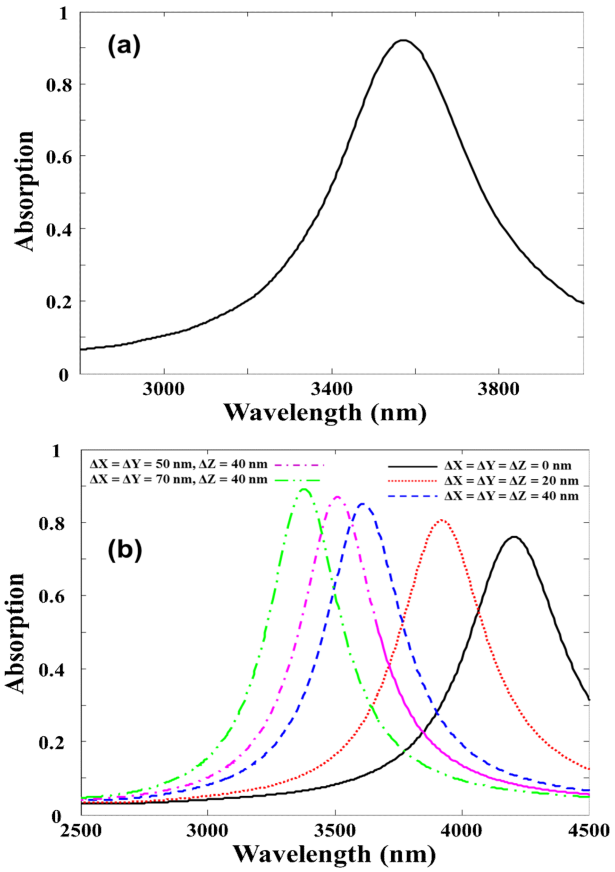

Fig. 2. (a) Simulated absorption spectral response of the MA and (b) the MA with a vertical nanogap for different under-cut depths.

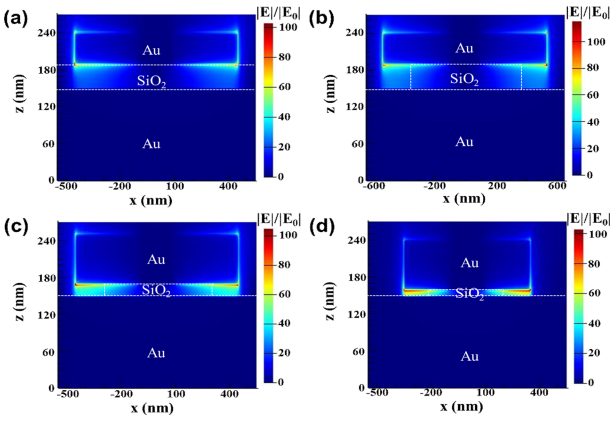

Fig. 3. (a) Cross-sectional views of the simulated electric near-field distributions at the plasmonic resonances for MA, (b) MA with a vertical nanogap of thickness 40 nm, (c) MA with a vertical nanogap of thickness 20 nm, and (d) MA with a vertical nanogap of thickness 10 nm.

respectively. From the results of near-field calculation, most of the enhanced near-fields are confined at the bottom of the Au cross nanoantenna, and the MA as well as the MA with a vertical nanogap illustrate a maximum field enhancement |E|/|E0| of approximately 100. The formation of the vertical nanogap of the MA by the under-cut structure increases the accessible sensing area beneath the Au cross nanoantenna. In addition, with the decrease in the thickness of the vertical nanogap (20 nm for Fig. 3 (c) and 10 nm for Fig. 3 (d)) as shown in Fig. 3 (c) and (d)), the enhanced near-field is confined and accumulated in the vertical nanogap and the enhanced near-field is extended along the side of bottom of the cross nanoantenna. This near-field distribution of the vertical nanogap suggests that the target molecular large spatial overlapping with the near-field can enhance the plasmonic-molecular coupling and increase the sensitivity of the SEIRA signal.

Figure 4 shows the simulated absorption spectral responses of the MA and the MAs with vertical nanogaps coated by the ODT monolayer. The black solid curves in Fig. 4 indicate the absorption spectral responses of the MA and the MAs with vertical nanogaps before the ODT monolayers are coated on them. The formation of the vertical nanogap of the MA and the decrease in the thickness of the vertical nanogap increase the sensitivity to the external refractive index. The ODT coating resulted in a resonance wavelength shift of 26 nm, 109 nm, 198 nm, and 423 nm for the MA as shown in Fig. 4 (a), the MA with a vertical nanogap of thickness 40 nm as shown in Fig. 4 (b), the MA with a vertical nanogap of thickness 20 nm as shown in Fig. 4 (c), and the MA

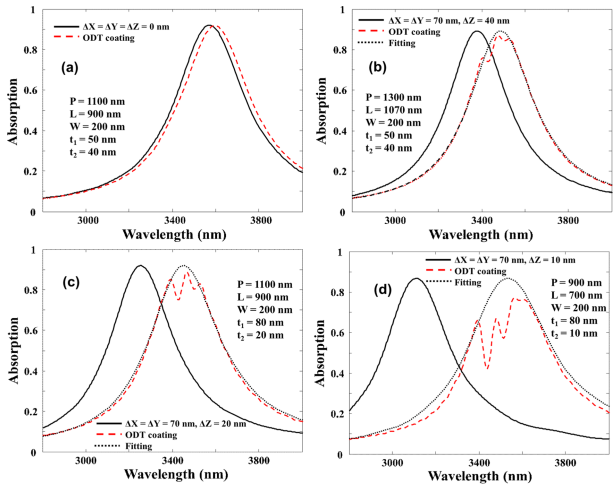

Fig. 4. (a) Simulated absorption spectral responses of the ODT-coated MA, (b) the ODT-coated MA with a vertical nanogap of thickness 40 m, (c) the ODT-coated MA with a vertical nanogap of thickness 20 m, and (d) the ODT-coated MA with a vertical nanogap of thickness 10 m.

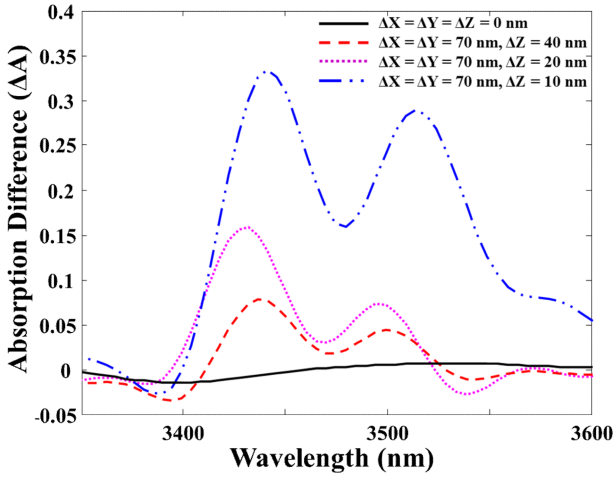

Fig. 5. Simulated absorption difference spectral responses of the MA (solid curve), the MA with a vertical nanogap of thickness 40 m (dashed curve), the MA with a vertical nanogap of thickness 20 m (dotted curve), and the MA with a vertical nanogap of thickness 10 m (dash-dotted curve).

with a vertical nanogap of thickness 10 nm as shown in Fig. 4 (d), respectively. Therefore, the MA with a vertical nanogap is designed to have its absorption resonance peak at a shorter wavelength compared with that of the MA, and the absorption resonances of the four ODT-coated MAs shift toward longer wavelengths and are formed at nearly the same wavelength. The simulated absorption spectral responses of the MAs with the vertical nanogaps except the MA shown in Fig. 4 (a) have vibrational signatures of ODT molecules at the two ODT vibrational wavelengths, where the absorption spectral response of the MA with a vertical nanogap of thickness 10 nm is more severely distorted.

To better illustrate the SEIRA detection signal, the absorption difference spectral responses ($\Delta A = A_{Fitting} - A_{ODT\ coating}$) are shown in Fig. 5. The absorption difference spectral response for the MA (black solid curve) does not contain the vibrational signatures of ODT molecules at the two ODT vibrational wavelengths. The peak-to-peak values of the differences in terms of absorption of the MA with a vertical nanogap of thickness 40 nm (red dashed curve) at the two ODT vibrational wavelengths are 11.3 % and 5.6 %. The blue dash-dotted curve in Fig. 5 shows that the peak-to-peak values of the differences in terms of absorption of the MA with a vertical nanogap of thickness 10 nm at the two ODT vibrational wavelengths are 36.2 % and 20.8 %. The enhanced SEIRA detection signal originates in the increased effective sensing area and integrated near-field distribution in the vertical nanogap of MA.

3. CONCLUSIONS

The monolayer detection of ODT molecules using an MA with a vertical nanogap was numerically demonstrated. The simulated results showed that creating a vertical nanogap of MA and decreasing the thickness of the vertical nanogap enhanced the plasmonic-molecular coupling and increased the sensitivity of the SEIRA signal. For the label-free optical sensing applications of the future, an MA with a vertical nanogap can provide a sensing platform to achieve ultrasensitive detection of a monolayer of molecules.

ACKNOWLEDGMENT

This work was supported by the Center for Advanced Meta-Materials (CAMM), funded by the Ministry of Science, ICT, and Future Planning as a Global Frontier Project (CAMM-No. 2014M3A6B3063707) and the Korea Institute of Machinery and Materials under Grant NK 211D.

REFERENCES

[1] P. R. Griffiths, J. A. De Haseth, and J. D. Winefordner, Fourier Transform Infrared Spectrometry, John Wiley & Sons, Hoboken, NJ, 2007.

[2] F. Neubrech, A. Pucci, T. W. Cornelius, S. Karim, A. Garcia-Etxarri, and J. Aizpurua, "Resonant plasmonic and vibrational coupling in a tailored nanoantenna for infrared detection," *Phys. Rev. Lett.*, Vol. 101, No. 15, pp. 157403-157406, 2008.

[3] E. Cubukcu, S. Zhang, Y. S. Park, G. Bartal, and X. Zhang, "Split ring resonator sensors for infrared detection of single molecular monolayers," *Appl. Phys. Lett.*, Vol. 95, No. 4, pp. 043113-043115, 2009.

[4] A. E. Cetin, D. Etezadi, and H. Altug, "Accessible near-fields by nanoantennas on nanopedestals for ultrasensitive vibrational spectroscopy," *Adv. Opt. Mat.*, Vol. 2, No. 9, pp. 866-872, 2014.

[5] C. Huck, A. Toma, F. Neubrech, M. Chirumamilla, J. Vogt, F. De Angelis, and A. Pucci, "Gold nanoantennas on a pedestal for plasmonic enhancement in the infrared," *ACS Photonics*, Vol. 2, No. 4, pp. 497-505, 2015.

[6] C. Huck, J. Vogt, M. Sendner, D. Hengstler, F. Neubrech, and A. Pucci, "Plasmonic enhancement of infrared vibrational signals: nanoslits versus nanorods," *ACS Photonics*, Vol. 2, No.10, pp. 1489-1497, 2015.

[7] K. Chen, T. D. Dao, S. Ishii, M. Aono, and T. Nagao, "Infrared aluminum metamaterial perfect absorbers for plasmon-enhanced infrared spectroscopy", *Adv. Func. Mat.*, Vol. 25, No. 42, pp. 6637-6643, 2015.

[8] A. Ishikawa and T. Tanaka, "Metamaterial absorbers for infrared detection of molecular self-assembled monolayers," *Sci. Rep.*, Vol. 5, No. 12570, pp. 1-7, 2015.
[9] P. A. Huidobro, M. Kraft, S. A. Maier, and J. B. Pendry, "Graphene as a tunable anisotropic or isotropic plasmonic metasurface," *ACS nano*, Vol. 10, No. 5, pp. 5499-5506, 2016.
[10] X. Ni, A. V. Kildishev, and A. V. Shalaev, "Metasurface holograms for visible light," *Nat. Commun.*, Vol. 4, No. 2807, pp. 1-6, 2013.
[11] N. Yu and F. Capasso, "Flat optics with designer metasurfaces," *Nat. Mater.*, Vol. 13, pp. 139-150, 2014.
[12] M. ElBadawe, T. S. Almoneef, and O. M. Ramahi, "A True Metasurface Antenna," *Sci. Rep.*, Vol. 6, No. 19268, pp. 1-8, 2016.
[13] N. F. Yu, P. Genevet, M. Kats, F. Aieta, J. P. Tetienne, J. P. Gapasso, and Z. Gaburro, "Light propagation with phase discontinuities: generalized laws of reflection and refraction," *Science*, Vol. 334, No. 6054, pp. 333-337, 2011.
[14] N. I. Landy, S. Sajuyigbe, J. J. Mock, D. R. Smith, and W. J. Padilla, "Perfect metamaterial absorber," *Phys. Rev. Lett.*, Vol. 100, No. 20, pp. 207402-207405, 2008.
[15] M. Pu, C. Hu, M. Wang, C. Huang, Z. Zhao, C. Wang, Q. Feng, and X. Xiangang, "Design principles for infrared wide-angle perfect absorber based on plasmonic structure," *Opt. Exp.*, Vol. 19, No. 18, pp. 17413-17420, 2011.
[16] Q. Feng, M. Pu, C. Hu, and X. Luo, "Engineering the dispersion of metamaterial surface for broadband infrared absorption," *Opt. Lett.*, Vol. 37, No. 11, pp. 2133-2135, 2012.
[17] A. Andryieuski and A. V. Lavrinenko, "Graphene metamaterials based tunable terahertz absorber: Effective surface conductivity approach," *Opt. Exp.*, Vol. 21, No. 7, pp. 9144-9155, 2013.
[18] L. V. Brown, K. Zhao, N. King, H. Sobhani, P. Nordlander, and N. J. Halas, "Surface-enhanced infrared absorption using individual cross antennas tailored to chemical moieties," *J. Am. Chem. Soc.*, Vol. 135, No. 9, pp. 3688-3695, 2013.
[19] C. D. Bain, E. B. Troughton, Y. T. Tao, J. Evall, G. M. Whitesides, and R. G. Nuzzo, "Formation of monolayer films by the spontaneous assembly of organic thiols from solution onto gold," *J. Am. Chem. Soc.*, Vol. 111, No. 1, pp. 321-335, 1989.
[20] X. Chen, C. Wang, Y. Yao, and C. Wang, "Plasmonic vertically coupled complementary antennas for dual-mode infrared molecule sensing," *ACS Nano*, Vol. 11, No. 8, pp. 8034-8046, 2017.